# Mechanical Properties of Layers Obtained by DC-Pulsed Plasma Nitriding on a Low-Alloy Steel (AISI 4140)

Luciano Dutrey,* Evangelina De Las Heras, Hernán G. Svoboda, Pablo A. Corengia

An industrial DC-pulsed plasma nitriding (DCPPN) equipment was used to obtain samples of an AISI 4140 low-alloy steel with five different configurations: substrate, substrate + diffusion zone, diffusion zone, substrate + diffusion zone + compound layer, and diffusion zone + compound layer. The microstructures of the samples were investigated by scanning electron microscopy and X-ray diffraction. Microhardness and tensile tests were performed, and the fracture mechanisms for the different materials were finally analyzed and discussed. The DCPPN produced an increase in the elastic modulus as well as in the yield strengths, together with a pronounce ductility loss, associated to the brittle intergranular fracture surface due to the nitride precipitation in the grain boundaries.

## Introduction

One of the greatest challenges imposed by the increasing technological progress is to develop new materials or to improve the existing ones in order to make them resistant to severely demanding working conditions.[1] In this sense, surface treatments can offer significant benefits, such us producing specific surface properties maintaining the bulk properties of the original material. Among them, plasma nitriding treatments have had a great development due to their advantages respect to conventional surface modification technologies:[2–4] they produce an effective combination of metallurgical properties, namely, increases of surface hardness, wear resistance, fatigue life, and, in certain cases, corrosion resistance;[5,6] it is an environmental friendly technology,[7] generates negligible volumetric changes, reduces the production costs, and improves the productivity. Some of the main applications, on a great diversity of substrates (steels, castings, sintered materials, titanium, and other alloys), are: cutting tools, matrices, valves, and other machine components. During the plasma nitriding treatment two zones are produced in low-alloy steels, namely, the so-called compound layer (adjacent to the surface), and the diffusion zone (underneath the previous one). The depth and the hardness of the diffusion zone depend on the alloy content and on the nitriding time and temperature.

The AISI 4140 is one of the most used low-alloy steels in nitrided structural elements. The process influence on the mechanical properties in bulk and on the variation of these from the surface toward the material core is a topic of great technological interest. Although there exist already a large amount of works devoted to diverse aspects of plasma nitriding in low-alloy steels, there is scarce information regarding systematic studies on the mechanical properties and on the deformation and

L. Dutrey, E. De Las Heras
Mechanics Research and Development Center, National Institute of Industrial Technology, Av. Gral. Paz 5445, B1650WAB, San Martín, Buenos Aires, Argentina
Fax: (+54) 11 4754 4072; E-mail: g-bio@inti.gob.ar
H. G. Svoboda
University of Buenos Aires, CONICET, Faculty of Engineering, INTECIN, Materials and Structures Laboratory, Las Heras 2214, 1427 Buenos Aires, Argentina
P. A. Corengia
Fundación INASMET-Tecnalia, Mikeletegi Pasealekua 2, E-20009 Donostia-San Sebastián, Guipúzcoa, Spain



DOI: 10.1002/ppap.200932404

*Table 1.* Chemical composition of the AISI 4140 low-alloy steel studied.

| Element | C | Mn | P | S | Si | Cr | Mo | Ni | Cu | Fe |
|---|---|---|---|---|---|---|---|---|---|---|
| wt.-% | 0.38 | 0.79 | 0.032 | 0.007 | 0.25 | 0.81 | 0.15 | 0.18 | 0.21 | Balance |

*Table 2.* Nitriding parameters.

| Time | Temperature | Pressure | Atmosphere | Tension | Current density | Pulse on/off |
|---|---|---|---|---|---|---|
| 4 h | 500 °C | 6 hPa | 75% $H_2$ + 25% $N_2$ | 750 V | $\sim 1.0^3$ A · $cm^{-2}$ | 20–700 μs |
| 15 h | 500 °C | 6 hPa | 75% $H_2$ + 25% $N_2$ | 750 V | $\sim 1.0^3$ A · $cm^{-2}$ | 20–700 μs |

*Table 3.* Different configurations studied.

| Series | Composition | Procedure |
|---|---|---|
| 1 | 100% substrate | Quenched and tempered |
| 2 | Substrate + diffusion zone | 4 h DCPPN + compound layer removed |
| 3 | 100% diffusion zone | 15 h DCPPN + compound layer removed |
| 4 | Substrate + diffusion zone + compound layer | 4 h DCPPN |
| 5 | Diffusion zone + compound layer | 15 h DCPPN |

fracture mechanisms for the different zones observed on nitrided materials.

The aim of the present work is to study the mechanical behavior of the different zones obtained by DC-pulsed plasma nitriding (DCPPN) on a Cr–Mo low-alloy steel, AISI 4140. Its objective is to provide a better understanding of this behavior through the analysis of the tensile properties and fracture modes in each region (for different fractions of substrate, diffusion zone, and compound layer).

## Experimental Details

The material used was a Cr–Mo low-alloy steel with the chemical composition shown in Table 1.

A 12.7 mm thickness AISI 4140 steel plate of 120 mm wide by 240 mm length was heat treated, applying an austenitization at 840 °C (for 25 min.), followed by an oil quenching and a tempering at 550 °C (for 2 h), in order to obtain a tempered martensite structure. Later on, the piece was machined and 1.5 mm thickness specimens were extracted using wire cutting in a Charmilles Roboform 550 electrical discharge machining (EDM) equipment. Afterwards, the specimens were ground to 1 mm. The DCPPN treatments were carried out under two different times, namely, 4 and 15 h[a]; the process parameters are given in Table 2. The compound layer was then removed from a group of samples in order to obtain the five different configurations, which are detailed in Table 3.

Once the five series of samples were obtained, a microstructural characterization was performed using a Philips SEM 505 scanning electronic microscope (SEM). The specimens for metallographic analyses were Ni electroplated — at 40 °C with a 1.5 mA current — to obtain a 10 μm thick protective layer, sectioned perpendicular to the treated surface, embedded in a mounting resin, ground with SiC paper, and polished using 1 μm alumina as the last step. The microstructure was revealed using 2% Nital (2 mL $HNO_3$ in 100 mL ethanol) and Vilella's (5 mL HCl + 1 g picric acid in 100 mL ethanol) — for the austenitic grain boundaries — etchants.

[a] The selection of these two treatment times was done in such a way that for the short process N could diffuse up to approximately a quarter of the sample thickness (~250 μm),[8,9] and for the long process up to approximately a half of the sample thickness (~500 μm).[8,9] Hence, samples were obtained therefore 50% of substrate and 50% of diffusion zone for the first case, and 100% of diffusion zone for the second case.

Microhardness profiles were carried out in a Shimadzu HMV-2000 equipment using loads of 0.25 N and a Vickers indenter. The compound layer and diffusion zone thicknesses were determined for each case applying the *Metals Handbook* method.[10] (i.e., where the surface hardness differ in more than 20 HV respect to the substrate).

The phases formed in the treated AISI 4140 were then characterized by X-ray diffraction (XRD) using a Cu-K$\alpha$ ($\lambda = 1.5406$ Å) radiation in a Philips-Rigaku X-ray diffractometer, with an average penetration depth in the material of 3 μm. A conventional $\theta/2\theta$ Bragg–Brentano symmetric geometry was used, from 30 to 90°, with a step size of 0.05° and a velocity of $1^\circ \cdot \text{min}^{-1}$.

Finally, for the different configurations, standardized tensile samples were machined by EDM and tensile tested according to ASTM E8M Standard in an Instron Series IX 4467 testing machine. The elastic modulus was determined by the extensometry.

In the last characterization step, the obtained fracture surfaces were analyzed by SEM and the failure modes for the different cases were determined.

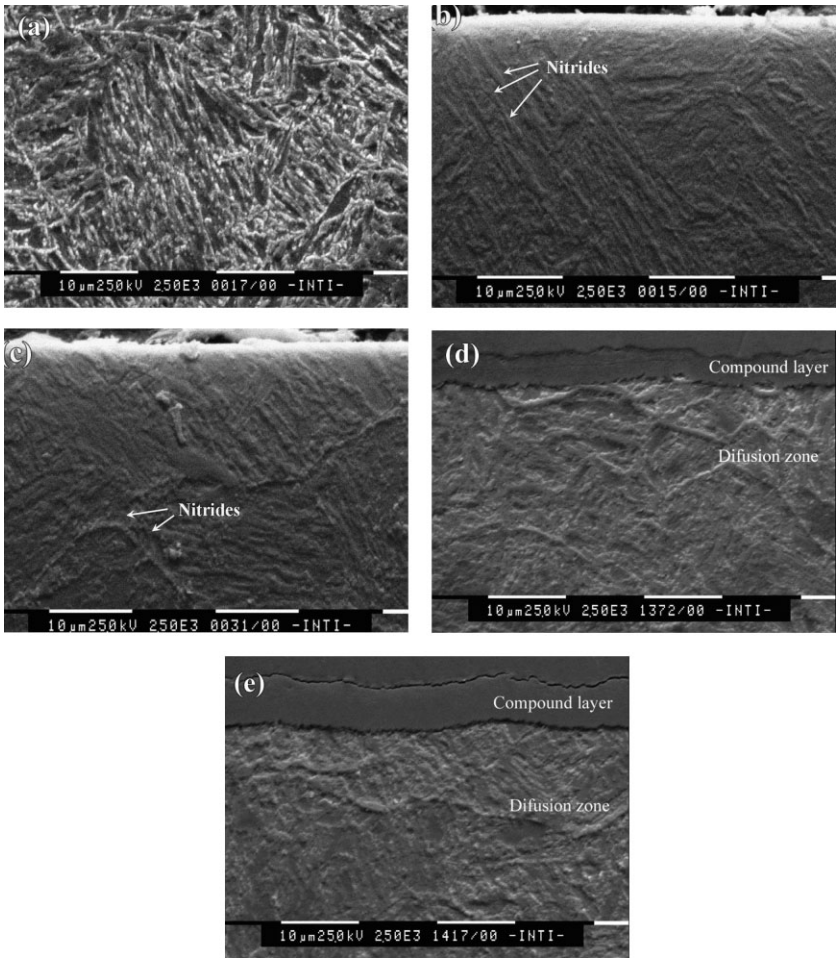


*Figure 1.* SEM micrographs of samples: (a) Series 1, (b) Series 2, (c) Series 3, (d) Series 4, and (e) Series 5.

## Results and Discussion

### Microestructural Characterization

Figure 1 shows SEM micrographs of Series 1–5 cross-sections. The tempered martensite microstructure corresponding to a sample of Series 1 after 2% Nital etching can be observed in Figure 1a. The microstructure of the diffusion zone without compound layer belonging to Series 2 is appreciated in Figure 1b. In this zone N can be in solution or forming nitrides.[7,8] In the microstructure corresponding to Series 3, the presence of nitrides precipitated at the grain boundaries can be seen (Figure 1c). The appearance of these precipitates was due to the longer treatment, which enables the introduction of a greater N amount, exceeding at a certain point the N solubility in the steel matrix.[11] As expected, the preferential precipitation places were the grain boundaries.[10,12] The adjacent zone to the free surface presented a higher N content that decreases toward the sample core. Microstructures of Series 4 and 5 are shown in Figure 1d and e (these samples are similar to Series 2 and 3, with the exception that the compound layer of the outer surface was conserved). In both cases, a continuous and uniform compound layer (unreactive to Nital etching) was appreciated. The thickness was approximately 4 μm for the short-treated sample and 6 μm for the long-treated one. Once more, nitride precipitation can be observed at the grain boundaries for Series 5.

Figure 2 shows the microhardness depth profiles, acquired on the samples cross-sections, of Series 4 and 5. The diffusion zone thickness, as expected, was greater in Series 3 and 5 than in Series 2 and 4. For the long treatment (15 h), this zone covered the whole material volume, reaching values of 40 HV above the substrate hardness (371 $HV_{0.25}$) in the sample center line region. In the short treatment (4 h), the thickness of the diffusion zone was around 230 μm. Therefore, it can be said that the two expected structural configurations were achieved, i.e., one consisting of a combination of diffusion zone plus substrate (plus compound layer): short treatment — Series 2 and 4, and the other consisting completely of diffusion



DOI: 10.1002/ppap.200932404

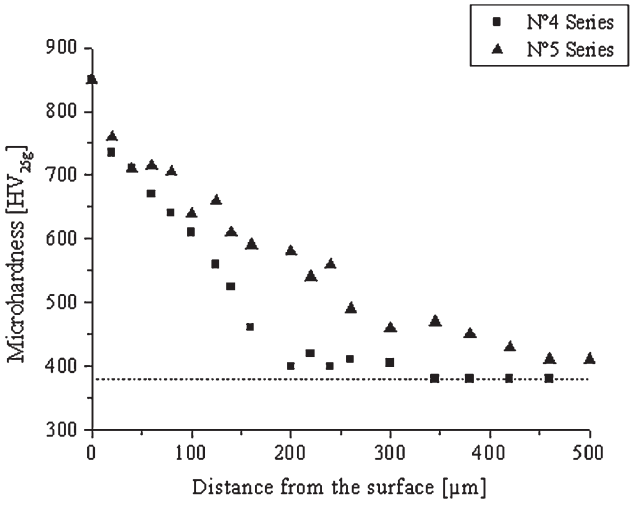


*Figure 2.* Microhardness depth profiles of the DCPPN samples for Series 4 and 5.

zone (plus compound layer): long treatment — Series 3 and 5. The surface hardness measured in Series 4 and 5 was practically the same for the 4 h treatment (851 $HV_{0.25}$) as for the 15 h treatment (845 $HV_{0.25}$), consistently with the values reported in the literature.[13,14]

In order to determine the present phases in the samples after the DCPPN process, an XRD analysis was performed on the surface. As reference, analyses of Series 1 samples — the substrate — were performed and peaks of only one component were identified, namely, $\alpha$-Fe.[10] For Series 2 samples — diffusion zone in the short treatment — , mainly peaks of $\alpha$-Fe were observed, which presented a broadening with respect to those observed for Series 1. In the literature, the introduction of compressive residual stresses related to the plasma nitriding process is reported as the reason for this broadening.[15] Nakata et al.[16] indicate that the peak broadening, associated to the presence of microstrains in the matrix, could be caused by the appearance of a coherent pre-precipitation phase. Nevertheless, it cannot be ignored that the compound layer elimination, performed by mechanical removal, could have introduced residual stresses in the material surface as well.[17] For Series 3 samples — diffusion zone in the long treatment — , peaks of $\alpha$-Fe were detected, with a more significant broadening with respect those of Series 1. In addition, small indications of nitride presence were observed. This fact was consistent with the micrographs, where the presence of precipitates was appreciated. For Series 4 samples — short treatment — , it was observed that the compound layer was constituted by the phases $\gamma'$-$Fe_4N$ and, to a lesser extent, $\varepsilon$-$Fe_{2-3}N$; in accordance with the reported data for this material compound layer.[10,13,14] Similarly, in Series 5 samples — long treatment — , the occurrence of $\gamma'$-$Fe_4N$ phase in the compound layer was confirmed, whereas $\varepsilon$-$Fe_{2-3}N$ has practically disappeared.[10,13,14]

## Mechanical Properties

The results obtained from the tensile tests on the five analyzed series are shown in Table 4. The numerical values correspond to an average of three tests per series.

The values obtained for the substrate are consistent with the data reported in the literature for this material. Regarding the nitrided series, 2–5, an increase of the resistance and of the elastic modulus was observed, along with a loss of ductility.

Series 2 and 4 — 4 h process — presented slight plastic deformation, more significant in the sample without compound layer. Series 3 and 5 — 15 h process — showed

*Table 4.* Tensile test results for the five tested series.

| Series | Yield strength 0.2% | | Tensile strength | | Elongation % $e_f\% = \frac{l_f - l_0}{l_0} \times 100$ | | Reduction of area to fracture % $q_f\% = \frac{A_0 - A_f}{A_0} \times 100$ | | Young modulus |
|---|---|---|---|---|---|---|---|---|---|
| | MPa | | MPa | | | | | | GPa |
| | Average | Deviation | Average | Deviation | Average | Deviation | Average | Deviation | E.E. |
| 1 | 1 126 | 23 | 1 269 | 18 | 17 | 1.5 | 47 | 1.9 | 201 |
| 2 | 1 288 | 24 | 1 432 | 26 | 1 | <1 | ~2 | <1 | 214 |
| 3 | 1 693 | 32 | 1 693 | 32 | <1 | <1 | ~1 | <1 | 220 |
| 4 | 1 284 | 24 | 1 314 | 25 | <1 | <1 | ~1 | <1 | 217 |
| 5 | 1 533 | 30 | 1 533 | 31 | <1 | <1 | ~1 | <1 | 224 |

E.E.: Electric extensometer.

practically a linear elastic behavior. For all nitrided samples, the elongation ($e_f$ %) and the reduction of area to fracture ($q_f$ %) were nearly zero, especially for the samples with compound layer. The ductility loss along with the tensile strength and the Young modulus increase in the nitrided samples are associated to the N diffusion into the $\alpha$-Fe crystalline matrix and to the nitrides precipitation.[18] In other words, the strength increase is produced by solid solution hardening and by coherent precipitates presence.[18] In addition, the strong ductility loss could be associated to the embrittlement induced by incoherent precipitation at grain boundaries.[18]

The maximum yield and tensile strength were obtained in Series 3 and the minimum in Series 1. In the short as well as in the long treatment, the samples with compound layer (4 and 5) showed lower tensile strength than their homologous without compound layer (Series 2 and 3, respectively). This was associated to the microcracks generation in the compound layer during the deformation process, as result of the different elastic modulus of each material fraction; i.e., the sample can be modeled as a composite working in an isodeformation condition.[12] During the tensile test, the compound layer with higher elastic modulus holds greater stresses, and due to its brittleness originates the cracked appearance and, finally, the propagation of the fracture front in the entire sample.

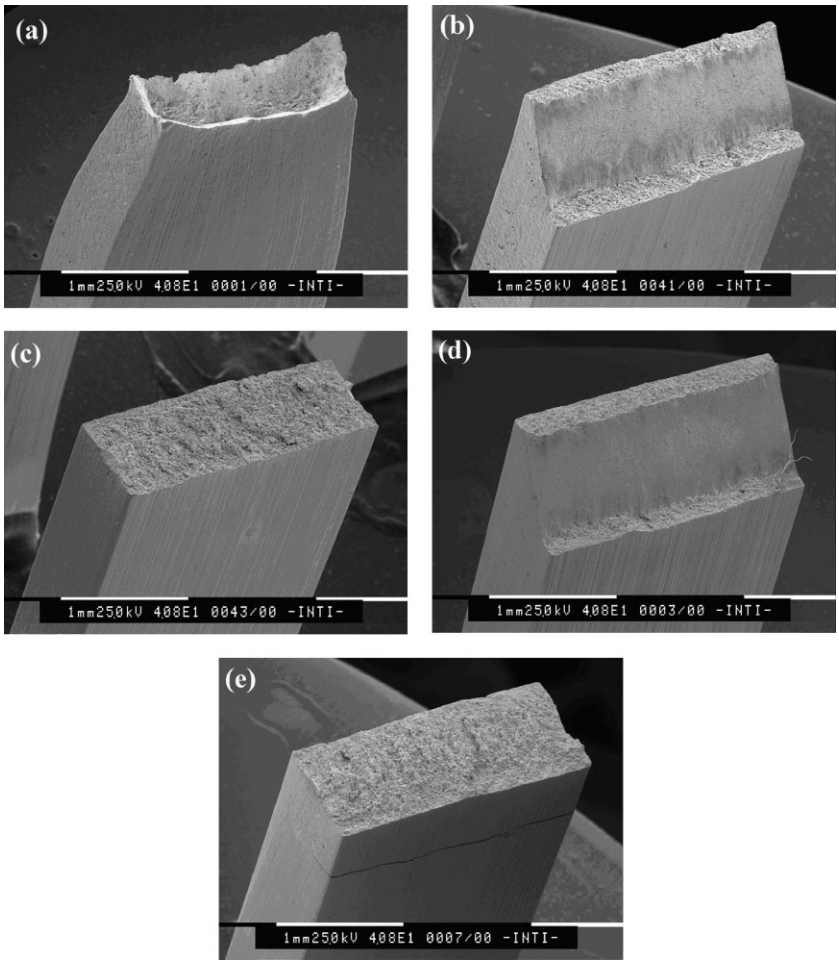


*Figure 3.* SEM images of the fracture surfaces: (a) Series 1, (b) Series 2, (c) Series 3, (d) Series 4, and (e) Series 5.

Concerning the elastic modulus, an increase was observed in the nitrided samples compared to the substrate, with higher values for the 15 h treatment than those for the 4 h one. This was associated to a crystalline structure modification due to the N solid solution. In addition, it was observed that, in both nitriding processes the modulus reaches higher magnitudes in the samples with compound layer. The presence of new phases in the compound layer, which present other crystalline structures and bond types — with higher elastic modulus — may explain the mentioned increase.

## Fracture Surfaces

Figure 3 shows SEM images of the fracture surfaces in perspective of the five studied series. Series 1 (Figure 3a), substrate, presented a typical cup and cone ductile fracture for rectangular sections,[19] in accordance with the tensile test results. A significant reduction of the cross-sectional fracture area is observed. Series 2 and 4 (Figure 3b and d), 4-h DCPPN, presented a mixed fracture, with the central part of the sample at 45° and flat outer regions. Although in this central fraction of the sample the material is relatively ductile — substrate —, the presence of the diffusion zone prevents the necking formation; therefore, inside the sample triaxiality could not take place. Hence, the central part fractured following the maximum shear stress plane.[12] Series 3 and 5 (Figure 3c and e), 15-h DCPPN, presented a classic brittle fracture with flat surface,[19] in accordance as well with the tensile test results. No reduction was appreciated in the cross-sectional fracture area.

The flat fracture zone thicknesses from Series 2 and 4 was measured on the micrographs, and corresponded well with the diffusion zone thicknesses determined by Vickers microhardness test.



DOI: 10.1002/ppap.200932404

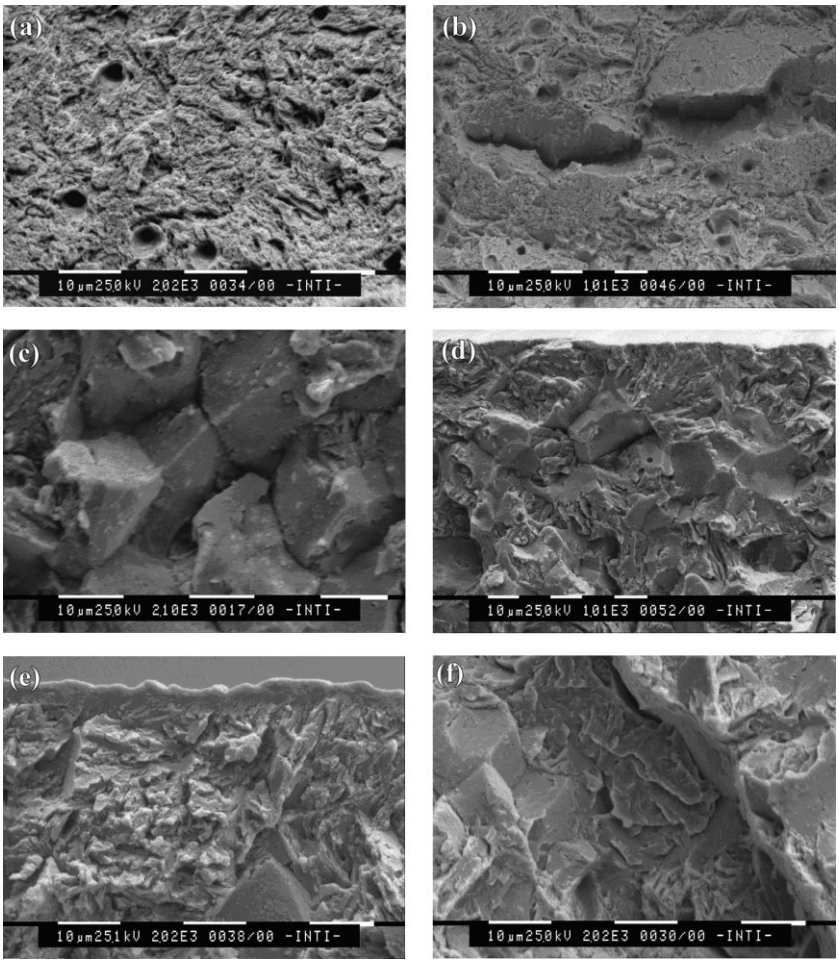


*Figure 4.* Micrographs of the fracture surface for: (a,b) Series 1, (c) Series 2, (d) Series 3, (e) Series 4, and (f) Series 5.

In Series 4 and 5 — samples with compound layer — secondary cracks on the surface were observed, which extended into the sample core perpendicular to the load direction. These cracks, were later seen, propagated through the grain boundaries; and its formation was associated to the embrittlement caused by nitride precipitation.

Figure 4 shows SEM images from the fractured surfaces observed on the different samples series. In Figure 4a, corresponding to Series 1, characteristic dimples from a ductile fracture can be appreciated,[19] and also microvoids related to the inclusions. In Figure 4b, Series 1, secondary microcracks and decohesion of the metallic matrix is observed. For Series 2, an intergranular fracture associated to nitride precipitation at grain boundaries is clearly distinguished (Figure 4c). This type of fracture was observed on the diffusion zones of the nitrided series. For Series 3, Figure 4d, a mixed fracture mode (with intergranular fracture) was observed in the sample edge zone — without compound layer. In Figure 4e, corresponding to Series 4, the fracture surface in the compound layer region can be appreciated, identifying a different morphology of brittle fracture for this zone. In Figure 4f, corresponding to Series 5, the presence of a few cleavage facets from a transgranular fracture can be seen (characteristic also of brittle fractures) along with intergranular fracture.

## Conclusion

The treated samples presented a compound layer and a diffusion zone, characteristic of the DCPPN.

An increase of the yield and tensile strength in the DCPPN samples compared to the untreated samples were observed, together with a pronounced ductility loss. The maximum strengths were obtained for samples with only diffusion zone. Samples with a compound layer showed lower yield and tensile strengths, associated to the microcracks generation during the deformation process.

The elastic modulus increased for the DCPPN samples. This increase was more noticeable for samples with compound layers.

Fracture surfaces for untreated samples presented a typical cup and cone ductile fracture for rectangular sections. Samples with substrate plus diffusion zone presented a mixed fracture, with the central part of the sample at 45° — following the maximum shear stress planes — and flat outer regions. Samples with diffusion zone presented a classic brittle fracture with flat surfaces.

The DCPPN samples showed intergranular fracture mode in the diffusion zone, related to nitride precipitation at grain boundaries. Few cleavage facets from transgranular fracture were also found, especially in the region close to the compound layer.

Acknowledgements: The authors are very grateful for the technical and financial assistance granted by the *Argentinean National Institute of Industrial Technology (INTI).* The authors would also like to thank the collaboration received from *Amorphous Solids Laboratory — FIUBA, INASMET-Tecnalia Foundation, IONAR SA, G. Meyer* from Balseiro Institute — CNEA, and *H. De Rosa* from FIUBA.

Received: January 10, 2009; Accepted: February 11, 2009; DOI: 10.1002/ppap.200932404

Keywords: mechanical properties; nitrides; pulsed plasma nitriding; steel

[1] T. Bell, K. Mao, Y. Sun, *Surf. Coat. Technol.* **1998**, *108–109*, 360.
[2] A. J. Hick, *Heat Treat. Met.* **2000**, *2*, 27.
[3] Y. Sun, T. Bell, *Mater. Sci. Eng. A* **1991**, *140*, 419.
[4] K. O. Legg, M. Graham, P. Chang, F. Rastagar, A. Gonzales, B. Sartwell, *Surf. Coat. Technol.* **1996**, *81*, 99.
[5] B. Edenhofer, *Heat Treat. Met.* **1974**, *1*, 23.
[6] E. J. Stefanides, *Design News* **1989**, *45*, 92.
[7] T. Bell, P. A. Dearnley, *Surf. Eng.* **1994**, *10*, 123.
[8] P. Corengia, G. Ybarra, C. Moina, A. Cabo, E. Broitman, *Surf. Coat. Technol.* **2005**, *200*, 2391.
[9] J. Lesage, D. Chicot, O. Bartier, M. A. Zampronio, P. E. V. de Miranda, *Mater. Sci. Eng.* **2000**, *282*, 203.
[10] ASM Committee on Gas Carburizing, Carbonitriding and Nitriding, in "*Heat Treating*", Metals Handbook, Vol. 4, 9th edition, C. A. Stickels, L. E. Byrnes, J. L. Dossett, R. L. Hughes, K. D. Gladden, J. A. Riopelle, R. D. Rogers, Eds., ASM Heat Treating Division Council, ASM Metals Park, OH 1982.
[11] E. Metin, O. T. Inal, *J. Mater. Sci.* **1987**, *22*, 2783.
[12] G. E. Dieter, Ed., "*Mechanical Metallurgy*", 3rd edition, Mc Graw-Hill, New York 1986.
[13] M. Karakan, A. Alsaran, A. Celik, *Mater. Charact.* **2003**, *49*, 241.
[14] F. Mahboubi, M. Samandi, D. Dunne, A. Bloyce, T. Bell, *Surf. Coat. Technol.* **1995**, *71*, 135.
[15] K. Genel, M. Demirkol, M. Capal, *Mater. Sci. Eng. A* **2000**, *279*, 207.
[16] K. Nakata, W. Yamauchi, K. Akamatsu, M. Ushio, *Surf. Coat. Technol.* **2003**, *174–175*, 1206.
[17] A. W. Warren, Y. B. Guo, M. L. Weaver, *Surf. Coat. Technol.* **2006**, *200*, 3459.
[18] D. Hong, M. Hillert, *Z. Metallkd.* **1991**, *82*, 310.
[19] G. W. Powell, in "*Failure Analysis and Prevention*", Metals Handbook, Vol. 11, 9th edition. *Prepared under the direction of ASM Handbook Committee*, G. W. Powell, S. E. Mahmound, Eds., ASM International, Metals Park, OH 1986.



DOI: 10.1002/ppap.200932404